TÜBİTAK

Turkish Journal of Chemistry

http://journals.tubitak.gov.tr/chem/

Research Article

Turk J Chem
(2015) 39: 563 – 575

doi:10.3906/kim-1411-21

The effect of temperature and concentration for methanol electrooxidation on Pt-Ru catalyst synthesized by microwave assisted route

Hilal DEMİR KIVRAK*
Chemical Engineering Department, Yüzüncü Yıl University, Van Turkey

Received: 10.11.2014 • **Accepted/Published Online:** 13.04.2015 • **Printed:** 30.06.2015

Abstract: At present, the methanol electrooxidation reaction (MOR) activities of carbon supported bimetallic Pt-Ru (M-PtRu@C) catalyst and monometallic Pt (M-Pt@C) catalysts prepared via microwave assisted polyol method and carbon supported Pt-Ru (P-PtRu@C) catalysts prepared by conventional polyol were examined to investigate the effect of the preparation method. These catalysts were characterized by X-ray diffraction, X-ray photo electron spectroscopy, and transmission electron microscopy (TEM). From TEM, the particle size of the M-PtRu@C catalyst was estimated as 3.54 nm. The MOR activities of these catalysts were examined at room temperature by cyclic voltammetry and chronoamperometry. Furthermore, stability measurements were performed on these catalysts to examine their long term stability. As a result, M-PtRu@C catalyst exhibited the best electrocatalytic activity and long term stability. Furthermore, MOR measurements at varying temperatures on M-PtRu@C catalyst showed turnover number reached its optimum value at 60 °C. At this temperature, M-PtRu@C catalyst could catalyze more methanol in the same period using the same number of sites compared to other applied temperatures.

Key words: Microwave assisted polyol, methanol electrooxidation, Pt-Ru, anode catalyst, fuel cells

1. Introduction

Direct methanol fuel cells (DMFCs) are popular power devices because methanol is easy to transport and widely available. Carbon supported Pt and Pt-Ru are still the electrocatalysts used most for DMFC electrodes.[1–10] Although the alloys with Ru show superior performance during the methanol electrooxidation reaction (MOR), the reaction mechanism over Pt is still not completely understood.[11–13] The complete MOR to CO_2 involves 6 electrons per molecule passing through anode to cathode.[11]

$$\text{Anode: } CH_3OH + H_2O \rightarrow CO_2 + 6H^+ + 6e^- \quad (1)$$

$$\text{Cathode: } 3/2\,0_2 + 6H^+ + 6e^- \rightarrow 3H_2O \quad (2)$$

$$\text{Overall: } CH_3OH + 3/2O_2 \rightarrow CO_2 + 2H_2O \quad (3)$$

The surface activity of nanoparticles is higher than that of the bulk materials because nanoparticles have a high surface to volume ratio. Hence, nanoparticles have potential applications in catalysis, strongly dependent on the size, shape, and impurities of metal nanoparticles. The rates of electrocatalytic oxidation of CO and methanol strongly depend on the structure of the catalyst. The electrocatalytic oxidation of CO on Pt single

*Correspondence: hilalkivrak@googlemail.com

crystals is a structure sensitive process and the rates were shown to increase in the order Pt (111) < Pt (100) < Pt (110).[14,15] It was reported that the MOR takes place via a dual pathway: (i) the direct pathway (soluble intermediates such as formic acid are formed) and (ii) the indirect pathway (CO adsorption occurs on the surface). It has been reported that MOR activities increase with decreasing particle size.[16]

The polyol method is commonly used for the synthesis of nanoparticles due to its advantages such as being surfactant free and inexpensive. This method also yields well-dispersed catalytic particles of small mean sizes. For this conventional polyol method, the synthesis is carried out by heating the reaction mixture at a temperature higher than 120 °C for several hours to reduce the metals.[17–25] As mentioned above, MOR activities are strongly size and shape dependent. Thus, the surface structure of the supporting materials has a great effect on the catalytic performance of the supported catalysts. Gu et al.[26] reported the MOR activities for three kinds of Ru nanocrystals with different morphologies and surface structures, namely triangular plates (TPs), capped columns (CCs), and nanospheres (NSs) as Pt@C > Pt-Ru CCs@C > Pt-Ru NSs@C ≈ Pt-RuTPs@C. From these results, one can understand that these nanocomposites exhibited dramatically different catalytic activity and stability. In addition, it is clear that the surface structure of the metal substrate influences the catalytic performance of the catalysts supported on the metal surface.[26]

Researchers concentrated on the effect of Ru addition on the MOR to improve MOR activity. Tripkovic et al.[27] also reported that the addition of Ru increases MOR activity. Waszczuk et al.[28] also studied the effect of Ru addition on MOR activity. Their results showed that the activity of this catalyst toward the MOR increased with the addition of Ru. Moreover, the activity of Pt-Ru catalyst was higher than that of the commercial one at the same Pt:Ru atomic ratios. Hydrogen adsorption/desorption characteristics of the homemade Pt-Ru and the commercial catalysts were significantly different. This behavior was attributed to (i) the role of ruthenium oxide present on the alloy particles at potentials of adsorbed hydrogen and methanol oxidation, (ii) the enhanced activity ruthenium atoms present at the edge of Ru nanosized islands for CO poison removal in comparison with the Pt-Ru alloy active sites.[28] Likewise, He and coworkers[29] worked on the effect of Ru addition and support on MOR activity. It was shown that the peak potential for methanol oxidation shifts to lower potential and the existing Ru can improve the stability and activity of electrodes for the MOR, attributed to the bifunctional mechanism of Ru to Pt.

The amount of catalyst loading is critical for the improvement of MOR activity. For instance, Wang et al.[30] reported that Pt-rich Pt-Ru alloys and PtRu@C catalysts with 20% Ru content exhibited the highest catalytic activity for the MOR.

The effect of concentration and temperature for the enhancement of the MOR was also studied by researchers. Tripkovic et al.[27] reported that the activity of Pt and Pt-Ru for the MOR is a strong function of pH, attributed to the pH competitive adsorption of oxygenated species with anions from supporting electrolytes. Moreover, Wang et al.[30] showed that MOR activity was suppressed at high concentrations of sulfuric acid due to sulfate-bisulfate adsorption.[30] Temperature has an enhanced effect on MOR activity. Tripkovic et al.[27] stated that an increase in temperature from 295 to 333 K increased the MOR activity of Pt and Pt-Ru catalysts by a factor of 5.

Microwave heating is a novel technique for preparing nanosized inorganic particles. The enhanced reaction kinetics, the formation of novel phases and morphologies, obtaining better and smaller size, and energy saving during the synthesis are the main advantages of the microwave synthesis route. Bensebaa et al.[31] reported that MOR activity was enhanced by employing Pt-Ru nanoparticles stabilized within a conductive polymer matrix prepared using microwave heating. Likewise, Harish and coworkers employed a polyol process activated

by microwave irradiation to prepare efficient Pt@C, Ru@C, and Pt-Ru@C electrocatalysts. Pt-Ru@C catalyst displayed high activity towards CO and MOR.[32] Furthermore, lower onset potentials and lower surface poisoning of MOR for Pt-Ru catalysts than those obtained on Pt@C catalysts were observed. Chu et al.[33] performed a study on microwave prepared Pt-Ru@C electrocatalysts with different mean particle sizes by modifying pH values during the preparation. It was reported that the particle size, composition, and catalytic activity of Pt-Ru@C catalyst are very sensitive to the pH value of the reducing solution. Although many studies were devoted to microwave synthesis, there are only a few studies on the application of MOR.[31,33–35] Many studies were dedicated to the effect of Ru addition, concentration, and temperature.[26–30] However, for microwave prepared catalysts, the effect of temperature and concentration has not been studied to date.

In the present study, the effect of microwave irradiation on MOR activity was examined. The effect of temperature and concentration on MOR activity for the microwave prepared catalyst was also investigated. MOR activities of carbon supported Pt-Ru (M-PtRu@C) catalyst and Pt (M-Pt@C) catalysts prepared via microwave assisted polyol method and carbon supported PtRu (P-PtRu@C) catalysts prepared by conventional polyol were explored. Furthermore, a comparative investigation was performed for MOR activity at different temperatures and methanol concentrations on M-PtRu@C catalyst. The main focus of this study was to investigate the effect of temperature and methanol concentrations on the MOR activity of M-PtRu@C catalyst.

2. Results and discussion

2.1. Characterization results

XRD patterns of M-Pt@C catalyst and M-PtRu@C and P-PtRu@C catalysts are illustrated in Figure 1, which reveal the structural information for the bulk of catalyst nanoclusters together with the carbon support. All samples show a diffraction peak at 25.8°, which is related to the (002) reflection of the structure of hexagonal carbon (JCPDS card no 75-1621). The other four peaks are characteristic of face-centered cubic (fcc) crystalline Pt (JCPDS card no 04-0802), corresponding to the (111), (200), (220), and (311) planes, at 2θ values of ca. 40°, 47°, 68°, and 82°, respectively. For these catalysts, Ru fcc peaks were not observed. The 2θ values of the (111) peak were 40.23° for M-Pt@C catalyst, 40.12° for P-PtRu@C catalyst, and 40.23° for M-PtRu@C catalyst. It is clear that the 2θ values of the (111) peak for M-PtRu@C catalyst experience peak shifts of –0.08°. The mean Pt particle diameters of the Pt-Ru@C catalysts were calculated from the Pt (111) diffraction peak via the Scherer equation. These particle size values of M-PtRu@C, P-PtRu@C, and M-Pt@C catalysts were 3.4, 6.1, and 8.4 nm, respectively. The mean Pt particle diameter decreased from 8.4 to 3.4 nm with increasing Ru content. This was attributed to Pt-Pt ensembles being separated by Ru particles inhibiting the agglomeration of Pt particles during the synthesis process.

XPS analyses were performed to investigate the chemical nature of these catalysts. Figure 2 shows spectra at high resolution of three possible oxidation states of platinum. The XPS spectrum for these catalysts indicated that binding energy (BE) for Pt $4f_{5/2}$ core level was 75.30 eV for M-Pt@C catalyst, 75.10 eV for P-PtRu@C catalyst, and 75.00 eV for M-PtRu@C catalyst. Furthermore, the BE values of $4f_{7/2}$ core level were 71.80 eV for M-Pt@C catalyst, 71.60 eV for P-PtRu@C catalyst, and 71.60 eV for M-PtRu@C catalyst. The Pt 4f XPS spectrum of M-PtRu@C catalyst experiences peak shifts of –0.20 eV for Pt $4f_{5/2}$ compared to the one of M-Pt@C catalyst, indicating an electronic structural change in Pt. Thus, one could note that the electronic structure and oxidation state of the catalyst changed when different preparation routes were employed. Furthermore, M-PtRu@C catalyst had the lowest BE values of Pt $4f_{5/2}$ and $4f_{7/2}$ core levels, meaning that Pt is in its metallic state in the presence of Ru. Binding energy goes up with the oxidation state of platinum,

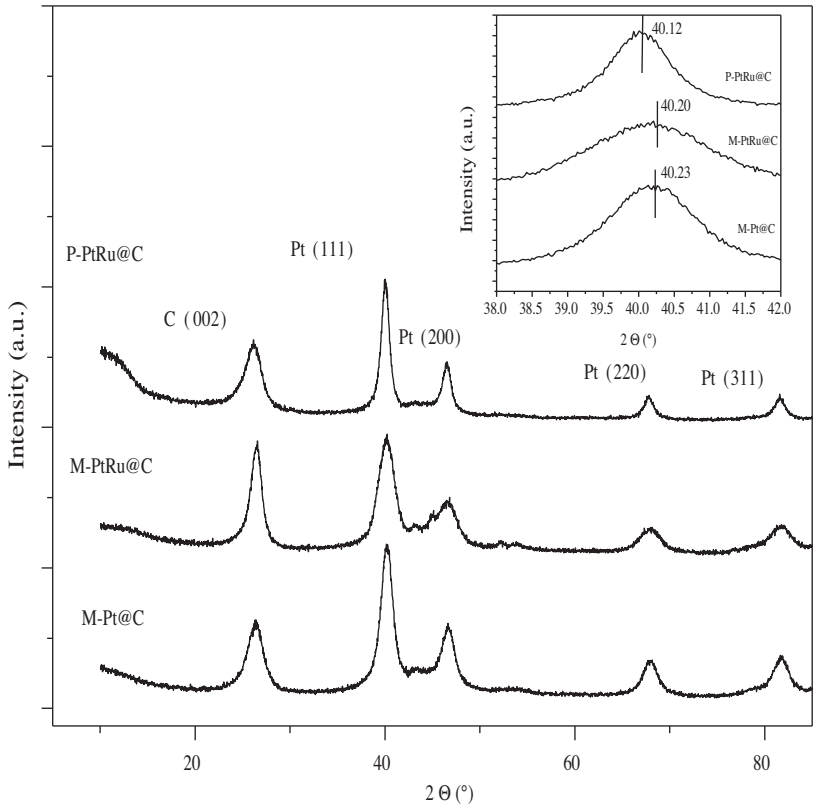

Figure 1. XRD patterns of M-PtRu@C, P-PtRu@C, and M-Pt@C electrocatalysts.

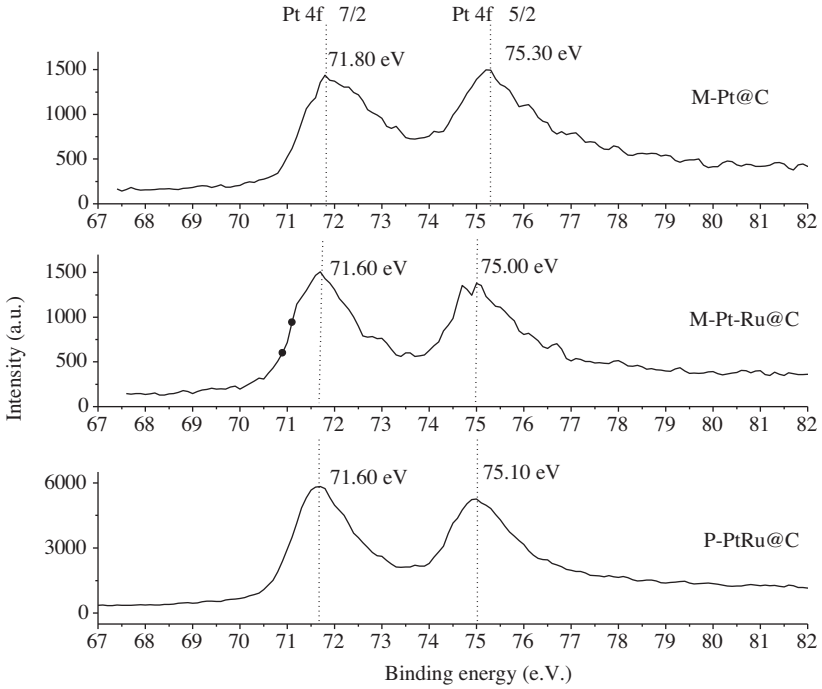

Figure 2. Pt 4f spectra of M-PtRu@C, P-PtRu@C, and M-Pt@C electrocatalysts.

because the 74 electrons in the Pt^{4+} ion feel a higher attractive force from the nucleus with a positive charge of 78 than the 76 electrons in Pt^{+2} or the 78 in the neutral Pt atom. The TEM image of the M-PtRu@C catalyst given in Figure 3a reveals that Pt-Ru nanoparticles were more homogeneously distributed. The mean particle diameters of this catalyst was obtained as 3.54 nm by counting over 300 particles, in agreement with the one obtained from XRD measurements (Figure 3b).[2,4,20,36,37]

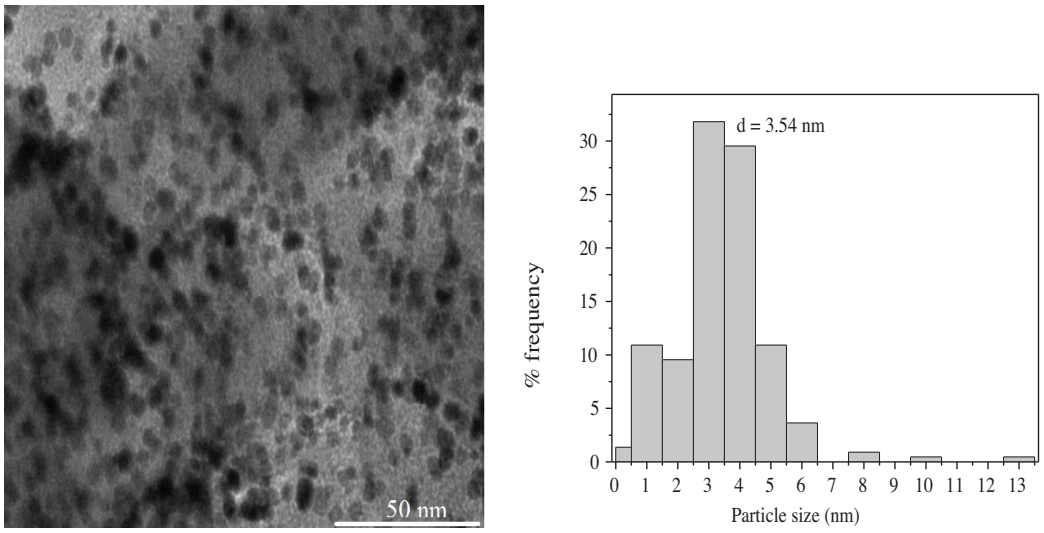

Figure 3. (a) TEM image for M-PtRu@C electrocatalysts and (b) Number frequency histograms showing particle size distribution.

2.2. Electrochemical measurements

The electrochemical activity of M-Pt@C, M-PtRu@C, and P-PtRu@C catalysts was measured by CV in 0.5 M H_2SO_4 solution (Figure 4). With the double layer and oxygen regions, the CV shape is similar to that of the Pt electrode, exhibiting several pairs of peaks corresponding to adsorption/desorption of hydrogen and oxygen containing species.[2] The characteristic value of charge density is associated with a monolayer of hydrogen adsorbed on polycrystalline platinum. Hence, one could conclude that the charge density of these catalysts is in the following order: M-PtRu@C > P-PtRu@C > M-Pt@C. One could ascribe this phenomenon to the fact that the reduction of metal particles could be achieved within seconds during microwave heating, leading to smaller particle size with relatively uniform particle size for M-PtRu@C catalyst.

MOR activity was evaluated on these catalysts in 0.5 M H_2SO_4 + 1 M CH_3OH at 50 mV s^{-1} scan rate. Typical polarization curves are shown in Figure 5 for these catalysts. During the forward scan, MOR commenced at 0.3–0.4 V and it was fully developed at 0.8 V. The MOR electrochemical activity of M-PtRu@C catalyst is greater than that of P-PtRu@C and M-Pt@C catalysts, due to its smaller particle size with relatively uniform particle size for M-PtRu@C catalyst. The maximum Pt mass normalized current values are 136 mA/mg Pt and 108 mA/mg Pt for M-PtRu@C and P-PtRu@C catalysts, respectively. The maximum Pt mass normalized current values were reported as 25–50 mA/mg Pt for Pt-Ru (E-TEK) commercial catalyst in the literature.[38,39] From this result, it is clear that the activity of M-PtRu@C electrocatalysts is 4 times higher than that of Pt-Ru (E-TEK) commercial catalyst. On the other hand, the activity of M-PtRu@C catalyst is nearly 3 times higher than the 54.1 mA/mg current value of Pt-Ru (25:1)@C catalyst prepared by polyol method in a previous study.[11] From Figure 4, one can see that the onset potentials of M-PtRu@C and M-Pt@C catalysts are 0.35 V

and 0.42 V, respectively. Gu et al.[26] reported that PtRu TPs@C possesses negative onset potential and higher activity compared to Pt@C catalyst. In conclusion, one could note that microwave irradiation increases the catalyst activity.[26] Comparing the activity of M-PtRu@C and M-Pt@C catalysts, one can see that the addition of the Ru improves MOR activity as previously reported in the literature.[27–29]

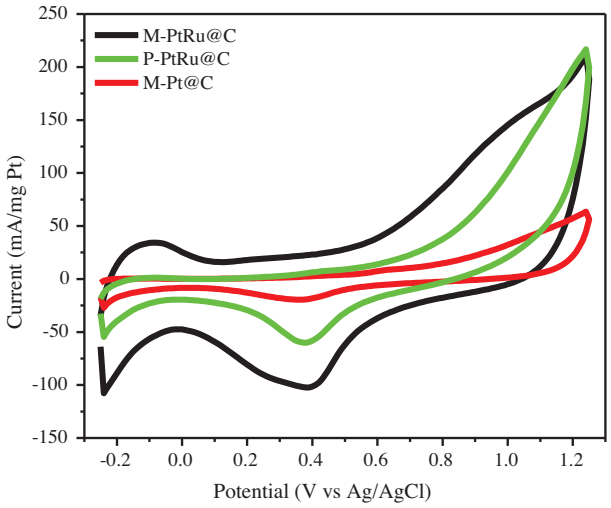

Figure 4. Cyclic voltammogram of M-PtRu@C, P-PtRu@C, and M-Pt@C electrocatalysts in 0.5 M H_2SO_4 at 25.0 °C (scan rate: 50 mV s^{-1}).

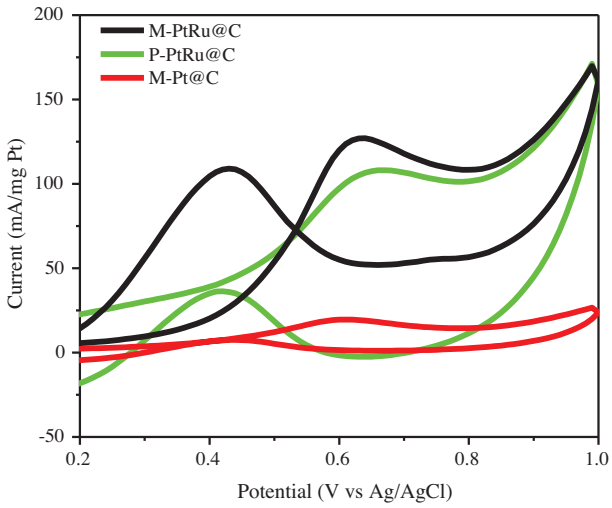

Figure 5. Cyclic voltammogram of M-PtRu@C, P-PtRu@C, and M-Pt@C electrocatalysts in 0.5 M H_2SO_4 + 1.0 M CH_3OH at 25.0 °C (scan rate: 50 mV s^{-1}).

Chronoamperomograms were taken of these catalysts in 0.5 M H_2SO_4 + 1.0 M CH_3OH solution at 0.6 V (Figure 6). There was a continuous current drop with time for MOR during the initial period because of the accumulation of intermediate species at the surface of catalysts. Apparently, deactivation of the catalysts proceeded very rapidly over the initial period of several minutes. After that, a slower steady decay was observed. It is clear that by the addition of Ru the initial current and steady state current increased. Similarly, Gu et al. reported that by the addition of Ru MOR activity of Pt particles was enhanced at different levels by introducing Ru nanoparticles.[26] M-PtRu@C catalyst showed the highest initial current and the highest current at the longer time, confirming that this catalyst had higher electrocatalytic activity and higher resistance to CO. Depending on these CA measurements, the turnover number (TON), the number of methanol molecules that react per catalyst surface site per second, was calculated by using the following equation:[40]

$$TON(molecules/s.site) = [I(mA/cm^2) \times NA]/[nF \times m_{Pt}(cm^2)], \quad (4)$$

where I is the steady state current density, n is the number of electrons produced by oxidation of 1 mole of methanol (n = 6), F is the Faraday constant (96,460.34 coulombs/mole), m is the mean atomic density of surface platinum on Pt (111) (1.51×10^{15} site/cm^{-2}), and NA *is* the Avogadro constant (6.02×10^{23}).[40]

For these measurements, TON values were calculated as 8.09×10^{-3} for M-PtRu and 2.87×10^{-3} for P-PtRu catalysts.

Stability measurements were conducted by LSV technique on these catalysts. Surface intermediates and CO form and bind readily and strongly on the surface, resulting in poisoning of catalyst. Thus, prior to LSV measurements, a surface pretreatment procedure was applied. Surface pretreatment was applied before methanol electrooxidation measurements. According to the surface pretreatment, potential was kept constant at

0.3 V for 1–100 s to poison the catalyst surface.[11] Then LSV measurements follow this pretreatment to explore MOR activity on the poisoned surface. These LSV measurements were performed to oxidize methanol on the poisoned surface. The maximum current values vs. poisoning time were read out from the LSV measurements. Then relative peak currents (maximum current × 100/ highest maximum current) were estimated.[11] The graph of relative peak currents vs. poisoning time is shown in Figure 7. The relative peak currents of M-PtRu@C catalyst slightly decreased to 85% over 200 s. However, these currents decreased 80% for P-PtRu@C catalyst and 68% for M-Pt@C catalyst. Based on these measurements, one could conclude that M-PtRu@C catalyst is more CO resistant than P-PtRu@C catalyst. This result indicates that the microwave synthesis route for the preparation of M-PtRu@C catalyst enhances the MOR activity of this catalyst.[11]

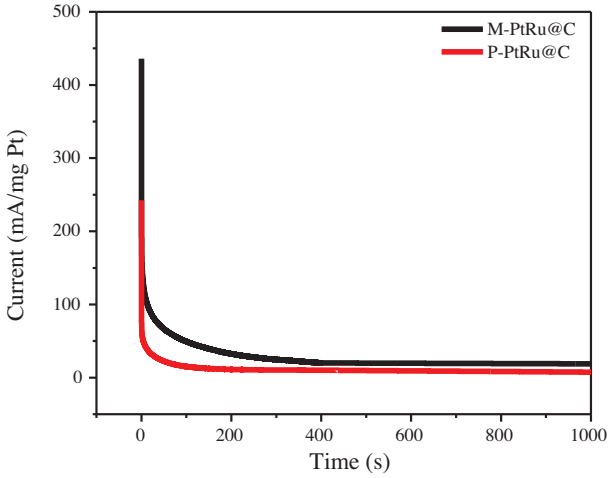

Figure 6. Chronoamperomogram of M-PtRu@C and P-PtRu@C electrocatalysts in 0.5 M H_2SO_4 + 1.0 M CH_3OH at 25.0 °C (applied potential: 0.6 V).

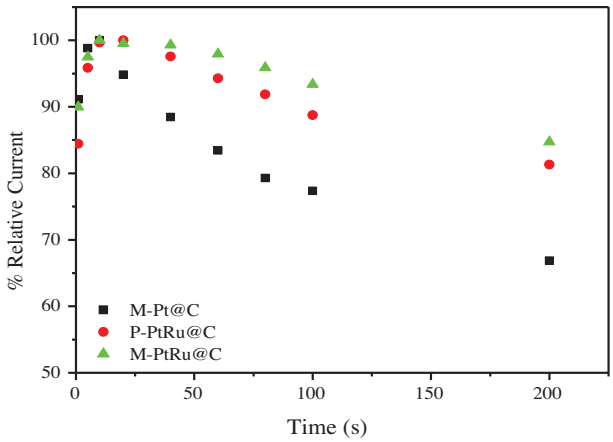

Figure 7. Relative current % vs. poisoning time values obtained from LSV measurements (scan rate: 100 mV s^{-1}) for M-PtRu@C, P-PtRu@C, and M-Pt@C electrocatalysts.

MOR activity measurements of M-PtRu@C catalyst at different temperatures (25–60 °C) were conducted by employing the CV technique in 0.5 M H_2SO_4 + 1.0 M CH_3OH. Figure 8 shows that the MOR current reached its optimum value at 60 °C. The peak current density at 60 °C was 2.3 times higher than that at 25 °C. Moreover, a negative shift of the onset oxidation potentials was observed with increasing temperature (Table).

Table. Comparison of electrocatalytic activity of MOR on M-PtRu@C catalyst at different temperatures.

Temperature (°C)	Onset potential (V)	Forward sweep		Reverse sweep		TON (molecules/s. Site)
		I_F (mA/mg Pt)	E (V)	I_R (mA/mg Pt)	E (V)	
25	0.35	136	0.62	108	0.43	8.09×10^{-3}
43	0.29	180	0.61	188	0.43	9.02×10^{-3}
60	0.23	312	0.62	440	0.49	1.33×10^{-2}

The onset potential was 0.35 V for 25 °C, 0.29 V for 43 °C, and 0.23 V for 60 °C. The decrease in the onset potential and increase in the forward maximum peak currents could be attributed to the fact that the MOR is thermally activated, which is in reasonable agreement with the literature results for Pt and Pt-Ru catalysts.[11,27] Tripkovic et al. reported that the onset of the MOR on Pt and PtRu electrodes shifted

significantly towards more negative potentials, attributed to an increase in the adsorption/dehydrogenation reaction step on Pt and in particular activation of the Ru.[27]

The MOR activities of M-PtRu@C catalyst at varying temperatures (25–60 °C) were also examined by CA technique. Chronoamperomograms were taken in 0.5 M H_2SO_4 + 1.0 M CH_3OH solution of these catalysts at 0.6 V (Figure 9). The highest initial currents and steady state currents were observed at 60 °C, in agreement with the CV measurements.

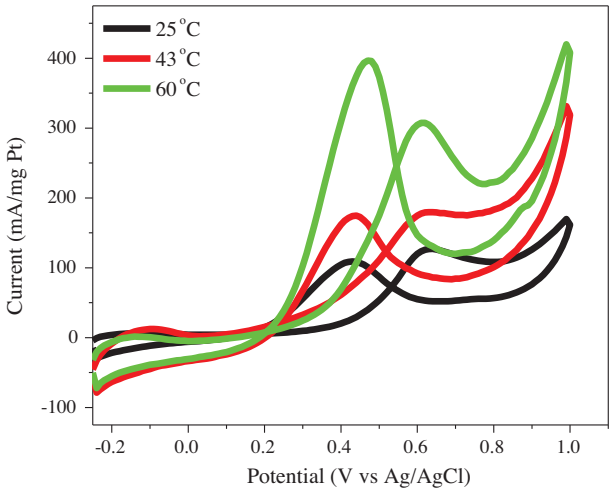

Figure 8. Cyclic voltammogram of M-PtRu@C electrocatalyst in 0.5 M H_2SO_4 + 1.0 M CH_3OH at varying temperatures (25–60 °C) (scan rate: 50 mV s^{-1}).

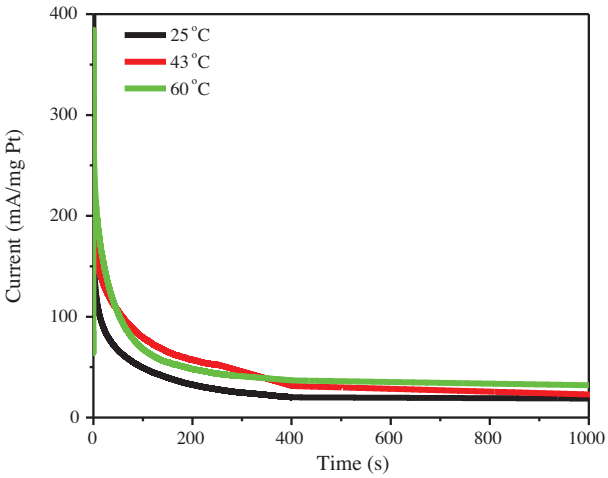

Figure 9. Chronoaperomogram of M-PtRu@C electrocatalyst in 0.5 M H_2SO_4 + 1.0 M CH_3OH at varying temperatures (25–60 °C) (scan rate: 50 mV s^{-1}, applied potential: 0.6 V).

For M-PtRu@C catalyst, TON values calculated at different temperatures (25–60 °C) are given in the Table. One can note that the MOR is thermally activated and the TON depends on the applied temperatures. For instance, the TONs are 8.09 × 10^{-3} at 25 °C, 9.02 × 10^{-3} at 43 °C, and 1.33 × 10^{-2} at 60 °C. It is clear that the largest TON was obtained at 60 °C, meaning that M-PtRu@C catalyst is able to catalyze more methanol at 60 °C in the same period using the same number of sites compared to the other applied temperatures, in agreement with the CV results.[40] The reaction pathway for the MOR on Pt-Ru catalysts at room temperature was previously proposed. In the first step, methanol adsorption is followed by methanol dehydrogenation and formation of CO adsorbed on the Pt surface, which are both surface intermediates and surface poisons. Furthermore, on the electrode surface, the removal of CO_{ads} at Pt sites proceeds though the reaction of CO_{ads} and OH_{ads} species. The final step is the reaction of OH_{ads} groups with neighboring methanolic residues adsorbed on Pt sites to give carbon dioxide.

$$Pt + CH_3OH \rightarrow PtCO_{ads} + 4H^+ + 4e^- \quad (5)$$

$$Ru + H_2O \rightarrow Ru(OH)_{ads} + H^+ + e^- \quad (6)$$

$$PtCO_{ads} + Ru(OH)_{ads} \rightarrow CO_2 + Pt + Ru + H^+ + e^- \quad (7)$$

The enhancement in methanol electrooxidation at high temperatures is due to the increase in OH adsorption and catalytic activity of Ru. It has been reported that temperature increase enhances OH adsorption and lowers

the OH adsorption potential on the Pt-Ru alloy surface. Thus, the rate of CO oxidation to CO_2 on the Pt surface increases at high temperatures.[7]

The effect of methanol concentration on the MOR activity of M-PtRu@C catalyst was examined at different methanol concentrations (0.05–2.0 M) in 0.5 M CH_3OH. The cyclic voltammograms at different acid concentrations on M-PtRu@C catalyst are given in Figure 10. The highest current value and the lowest onset potential were obtained at 1 M methanol concentration. It is clear that the oxidation current increased with concentration up to 1.0 M and then decreased at higher methanol concentrations.

Chronoamperomograms taken in 0.5 M H_2SO_4 + (0.05–2.0 M) CH_3OH solution and given in Figure 11 indicate that the highest initial currents and steady state currents were observed at 1 M, in agreement with the CV measurements. TONs were also calculated depending on the steady state current values obtained from chronoamperomograms as 3.30×10^{-3} for the measurement in 0.5 M H_2SO_4 + 0.05 M CH_3OH, 3.41×10^{-3} for the measurement in 0.50 M H_2SO_4 + 0.50 M CH_3OH, 8.40×10^{-3} for the measurement in 0.5 M H_2SO_4 + 1.0 M CH_3OH, and 4.35×10^{-3} for the measurement in 0.5 M H_2SO_4 + 2.00 M CH_3OH solutions. It is clear that TONs increase up to 1.0 M CH_3OH concentration and start to decrease, meaning that the number of active sites decreases on the electrode due to higher methanol concentration. At higher concentrations, the reaction was diffusion controlled. At high concentrations, in the reaction medium, the excess amount of methanol can lead to excess production of reaction intermediates such as CO adsorbed on the surface. The adsorption of CO decreases the number of active sites on the electrode.

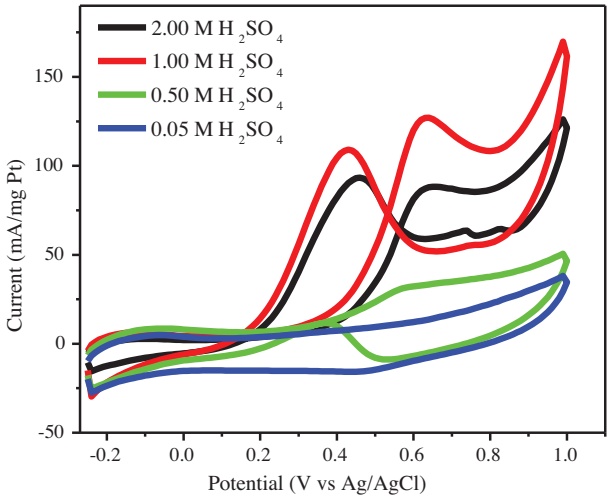

Figure 10. Cyclic voltammogram of M-PtRu@C in 0.5 M H_2SO_4 + different CH_3OH (0.05–2.0 M) concentrations at 25.0 °C (scan rate: 50 mV s^{-1}, applied potential: 0.6 V).

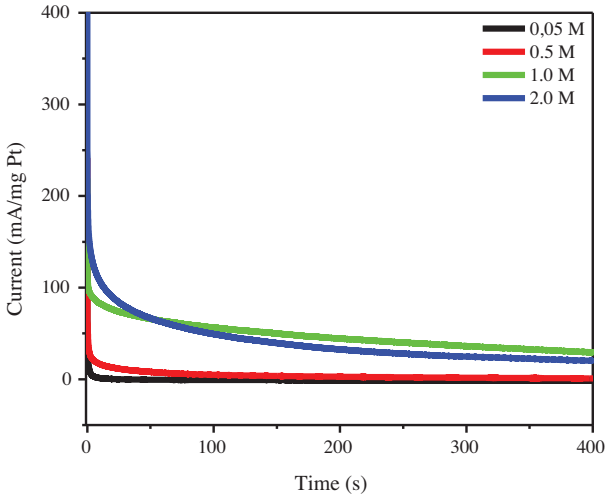

Figure 11. Chronoamperomogram of M-PtRu@C electrocatalyst in 0.5 M H_2SO_4 + different CH_3OH (0.05–2.0 M) concentrations at 25.0 °C (scan rate: 50 mV s^{-1}, applied potential: 0.6 V).

Stability measurements were also conducted by LSV technique on M-PtRu@C catalyst to explore its MOR stability at different concentrations. As mentioned above, the relative peak currents (maximum current × 100/highest maximum current) were estimated. The graph of relative peak currents vs. poisoning time is shown in Figure 12. Relative peak currents of M-PtRu@C catalyst altered depending on the methanol concentration. One can see that relative current values belonging to M-PtRu@C catalyst decreased with increasing methanol concentration, indicating that a small amount of poisoning occurs on the platinum sites

while methanol concentration increases. The excess amount of methanol can lead to excess production of reaction intermediates such as CO adsorbed on the surface in the reaction medium, in agreement with the CV and CA measurements.[11,40]

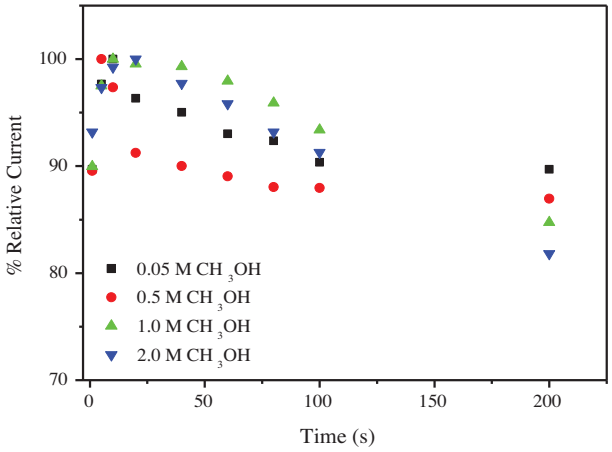

Figure 12. Relative current % vs. poisoning time values obtained from LSV measurements performed in 0.5 M H_2SO_4 + different CH_3OH (0.05–2.0 M) concentrations at 25.0 °C (scan rate: 100 mV s^{-1}) for M-PtRu@C electrocatalyst.

In conclusion, the study of the microwave assisted preparation, characterization, and employment of carbon supported Pt-Ru and Pt catalysts led to the following conclusions and insights:

- Pt-Ru nanoparticles can be easily prepared from the co-reduction of corresponding platinum and ruthenium salts by microwave assisted polyol method.
- Microwave assisted synthesized Pt-Ru nanoparticles are a highly efficient catalyst for MOR activity compared to Pt-Ru catalysts prepared via the conventional polyol method.
- Microwave assisted synthesized Pt-Ru nanoparticles provide TON values as 8.09 × 10^{-3} at 25 °C, 9.02 × 10^{-3} at 43 °C, and 1.33 × 10^{-2} at 60 °C, revealing that microwave assisted Pt-Ru nanoparticles are able to catalyze more methanol at 60 °C in the same period using the same number of sites compared to other applied temperatures.
- Microwave is a facile method for the preparation of nanoparticles. This method could be regarded as promising for the preparation of anode catalysts for proton exchange membrane fuel cells.

3. Experimental

3.1. Materials

$RuCl_3.xH_2O$ (35%–40% Ru), $H_2PtCl_6.6H_2O$ (38%–40% Pt), ethylene glycol (99.5%), CH_3OH (99.99%), and H_2SO_4 (95-97%), purchased from Sigma-Aldrich, were used in the experiments. Carbon (Vulcan XC72 R) (particle size: 50 nm, purity > 99.9%, density: 1.8 g/cm^3) was obtained from Cabot Corporation. Nafion 117 solution (5%) was obtained from Aldrich.

3.2. Preparation and characterization of electrocatalysts

M-Pt@C and M-PtRu@C catalysts were prepared by microwave assisted and conventional polyol methods. Deposition of Pt-Ru nanoparticles on carbon was achieved by reduction of $RuCl_3.xH_2O$ (35%–40% Ru) and $H_2PtCl_6.6H_2O$ (38%–40% Pt) metal salts with ethylene glycol and glycerol. Metal salts, KBr, and NaOH were all dissolved in glycerol and ethylene glycol. Carbon support was firstly impregnated with $H_2PtCl_6.6H_2O$ and $RuCl_3.xH_2O$, and 0.12 M KBr (stabilizer) solutions were added. The resulting mixture was treated in an ultrasonic bath for 1 h. Next, 5 mL of 0.05 M NaOH was added drop by drop under magnetic stirring. Microwave reactor tubes containing the resulting solution was put into a microwave reactor (Anton Paar monowave 300) and heated for 2 min at 130 °C. Finally, the samples were filtered, washed with distilled water and ethanol, and dried in an oven at 60 °C. Pt-Ru catalyst was prepared at 25:1 atomic ratio. In the conventional polyol method, the only difference is the heating procedure. The resulting solution obtained after metal impregnation and NaOH addition was refluxed under Ar atmosphere for 2 h at 120 °C. Next, the same procedure for filtration, washing, and drying was followed. Pt metal loading was 10% per gram support for all the catalysts.

XRD patterns were measured on a Bruker D8 ADVANCE X-ray diffractometer using Cu Kα-ray radiation (λ = 1.5405 Å) operating at 30 kV and 15 mA. XRD patterns were recorded between 2θ = 10.0 and 85.0° with 0.05° intervals and 1° data collection velocity in 1 min.

Surface characterization of catalysts for the oxidation states of the surface species by X-ray photoelectron spectroscopy (XPS) was performed. The X-ray photoelectron spectra was obtained using Mg-Kα (hv = 1253.6 eV) unmonochromatized radiation with a SPECS spectrometer. The charging effects were corrected by using the C 1s peak as reference for all samples at a binding energy (BE) of 284.8 eV. The size of the catalysts was studied by transmission electron microscopy (TEM) at 120 kV. Samples were prepared by dropping one drop of dilute suspension on the copper coated carbon TEM grid and the solvent was then dried. The surface area of the catalysts was predicted by assuming spherical particles.

3.3. Preparation of working electrode

The surface of the glassy carbon electrode was polished with alumina before electrode preparation. For the electrode preparation, 5 mg of catalyst was dispersed in 1 mL of Aldrich 5% Nafion solution to obtain the catalyst ink. Then 5 μL of the ink was spread on the surface of the glassy carbon electrode. The electrode was dried at room temperature to remove the solvent.

3.4. Electrochemical measurements

Electrochemical measurements were carried out in a conventional three-electrode cell with Pt wire as a counter electrode and Ag/AgCl (sat. KCl) as a reference electrode with a CHI 660E potentiostat. The working electrode was a glassy carbon disk with a diameter of 3.0 mm held in a Teflon cylinder. Cyclic voltammetry (CV) and chronoamperometry (CA) techniques were performed on M-Pt@C, M-PtRu@C, and P-PtRu@C catalysts. Cyclic voltammograms and chronoamperomograms were recorded in 0.5 M H_2SO_4 + 1 M CH_3OH solution on these catalysts. During the experiments, ultrahigh purity Ar was introduced into the electrochemical cell above the solution as a protection atmosphere. Prior to each experiment, the electrode surface was activated in 0.5 M H_2SO_4. First of all, CV measurements were obtained in 0.5 M H_2SO_4 with a scan rate of 50 mV s^{-1}. To examine the MOR activity, CV was recorded between –0.2 V and 1.0 V with a scan rate of 50 mV s^{-1} at 25 °C in H_2SO_4 + CH_3OH solutions prepared at 0.5 M H_2SO_4 and 0.05–2.00 M CH_3OH concentrations. CA was performed in 0.5 M H_2SO_4 +1 M CH_3OH solution at 0.6 V for 200 s with 1000 s pulse width and 2 s quiet

times. MOR measurements at different temperatures (25.0–60.0 °C) on M-Pt@C, M-PtRu@C, and P-PtRu@C catalysts were carried out by CV and CA in 0.5 M H_2SO_4 + 1.0 M CH_3OH solution. Stability measurements were performed via linear sweep voltammetry (LSV) on M-Pt@C, M-PtRu@C, and M-PtRu@C catalysts. Prior to LSV measurements, potential was held at 0.3 V for 1–200 s. Then LSV measurements were performed in 0.5 M H_2SO_4 and 0.05–2.00 M CH_3OH solution at 100 mV s^{-1} scan rate. Details of this procedure were given in our previous study.[11]

Acknowledgments

The CHI 660E potentiostat employed in electrochemical measurements was purchased from the Scientific and Technological Research Council of Turkey (TÜBİTAK) project (project no: TÜBİTAK 113Z249). The chemicals were purchased from administrative units of the scientific research projects of Selçuk University (project no: S.U. 11401131). XRD measurements were performed at Selçuk University central laboratory. XPS and TEM measurements were conducted at METU central laboratory.

References

1. Zhao, G. Y.; Xu, C. L.; Guo, D. J.; Li, H.; Li, H. L. *J. Power Sources* **2006**, *162*, 492–496.
2. Raman, R. K.; Shukla, A. K.; Gayen, A.; Hegde, M. S.; Priolkar, K. R.; Sarode, P. R.; Emura, S. *J. Power Sources* **2006**, *157*, 45–55.
3. Wang, Z. B.; Yin, G. P.; Shi, P. F. *J. Electrochem. Soc.* **2005**, *152*, A2406–A2412.
4. Prabhuram, J.; Zhao, T. S.; Liang, Z. X.; Chen, R. *Electrochim. Acta* **2007**, *52*, 2649–2656.
5. Peng, F.; Zhou, C. M.; Wang, H. J.; Yu, H.; Liang, J. H.; Yang, J. A. *Catal. Commun.* **2009**, *10*, 533–537.
6. Liu, H. S.; Song, C. J.; Zhang, L.; Zhang, J. J.; Wang, H. J.; Wilkinson, D. P. *J. Power Sources* **2006**, *155*, 95–110.
7. Jha, N.; Reddy, A. L. M.; Shaijumon, M. M.; Rajalakshmi, N.; Ramaprabhu, S. *Int. J. Hydrogen Energy* **2008**, *33*, 427–433.
8. Steigerwalt, E. S.; Deluga, G. A.; Cliffel, D. E.; Lukehart, C. M. *J. Phys. Chem. B* **2001**, *105*, 8097–8101.
9. Bayrakçeken, A. *Turk. J. Chem.* **2014**, *38*, 309–316.
10. Ye, L.; Ou, Z.; Meng, D.; Yuan, M.; Fang, Y.; Kadish, K. M. *Turk. J. Chem.* **2014**, *38*, 994–1005.
11. Sahin, O.; Kivrak, H. *Int. J. Hydrogen Energy* **2013**, *38*, 901–909.
12. Kivrak, H.; Kuliyev, S.; Tempel, H.; Schneider, J.; Uner, D. *Int. J. Chem. Reactor Eng.* **2011**, *9*, A36–A45.
13. Tian, Z. Q.; Jiang, S. P.; Liang, Y. M.; Shen, P. K. *J. Phys. Chem. B* **2006**, *110*, 5343–5350.
14. Lebedeva, N. P.; Rodes, A.; Feliu, J. M.; Koper, M. T. M.; van Santen, R. A. *J. Phys. Chem. B* **2002**, *106*, 9863–9872.
15. Lebedeva, N. P.; Koper, M. T. M.; Feliu, J. M.; van Santen, R. A. *J. Phys. Chem. B* **2002**, *106*, 12938–12947.
16. Lai, S. C. S.; Lebedeva, N. P.; Housmans, T. H. M.; Koper, M. T. M. *Top. Catal.* **2007**, *46*, 320–333.
17. Jiang, L. H.; Zhou, Z. H.; Zhou, W. J.; Wang, S. L.; Wang, G. X.; Sun, G. Q.; Xin, Q. *Chem. J. Chinese Univ-Chinese* **2004**, *25*, 1511–1516.
18. Kowal, A.; Gojkovic, S. L.; Lee, K. S.; Olszewski, P.; Sung, Y. E. *Electrochem. Commun.* **2009**, *11*, 724–727.
19. Susut, C.; Nguyen, T. D.; Chapman, G. B.; Tong, Y. *Electrochim. Acta* **2008**, *53*, 6135–6142.
20. Liu, Z. L.; Ling, X. Y.; Guo, B.; Hong, L.; Lee, J. Y. *J. Power Sources* **2007**, *167*, 272–280.
21. Lee, W. D.; Lim, D. H.; Chun, H. J.; Lee, H. I. *Int. J. Hydrogen Energy* **2012**, *37*, 12629–12638.

22. Zhou, Z. H.; Zhou, W. J.; Wang, S. L.; Wang, G. X.; Jiang, L. H.; Li, H. Q.; Sun, G. Q.; Xin, Q. *Catal. Today* **2004**, *93–95*, 523–528.
23. Jiang, L. H.; Sun, G. Q.; Zhou, Z. H.; Xin, Q. *Catal. Today* **2004**, *93–95*, 665–670.
24. Liu, Z. L.; Hong, L.; Tay, S. W. *Mater. Chem. Phys.* **2007**, *105*, 222–228.
25. Wang, G. X.; Sun, G. Q.; Zhou, Z. H.; Liu, J. G.; Wang, Q.; Wang, S. L.; Guo, J. S.; Yang, S. H.; Xin, Q.; Yi, B. L. *Electrochem. Solid State Lett.* **2005**, *8*, A12–A16.
26. Gu, J.; Liu, W. C.; Zhao, Z.-Q.; Xu-Len, G.; Zhu, W.; Zhang, Y. W. *Inorg. Chem. Front.* **2014**, *1*, 109–117.
27. Tripkovic, A. V.; Popovic, K. D.; Grgur, B. N.; Blizanac, B.; Ross, P. N.; Markovic, N. M. *Electrochim. Acta* **2002**, *47*, 3707–3714.
28. Waszczuk, P.; Solla-Gullon, J.; Kim, H. S.; Tong, Y. Y.; Montiel, V.; Aldaz, A.; Wieckowski, A. *J. Catal.* **2001**, *203*, 1–6.
29. He, Z. B.; Chen, J. H.; Liu, D. Y.; Zhou, H. H.; Kuang, Y. F. *Diamond Relat. Mater.* **2004**, *13*, 1764–1770.
30. Wang, H.; Alden, L. R.; DiSalvo, F. J.; Abruna, H. D. *Langmuir* **2009**, *25*, 7725–7735.
31. Bensebaa, F.; Farah, A. A.; Wang, D. S.; Bock, C.; Du, X. M.; Kung, J.; Le Page, Y. *J. Phys. Chem. B* **2005**, *109*, 15339–15344.
32. Harish, S.; Baranton, S.; Coutanceau, C.; Joseph, J. *J. Power Sources* **2012**, *214*, 33–39.
33. Chu, Y. Y.; Wang, Z. B.; Jiang, Z. Z.; Gu, D. M.; Yin, G. P. *Fuel Cells* **2010**, *10*, 914–919.
34. Zhao, D.; Shi, M. Q.; Liu, W. M.; Chu, Y. Q.; Ma, C. A. *Micro Nano Lett.* **2014**, *9*, 50–54.
35. Chen, W. X.; Zhao, J.; Lee, J. Y.; Liu, Z. L. *Chem. Lett.* **2004**, *33*, 474–475.
36. Rodriguez-Nieto, F. J.; Morante-Catacora, T. Y.; Cabrera, C. R. *J Electroanal. Chem.* **2004**, *571*, 15–26.
37. Zhou, W. J.; Zhou, Z. H.; Song, S. Q.; Li, W. Z.; Sun, G. Q.; Tsiakaras, P.; Xin, Q. *Appl. Catal., B* **2003**, *46*, 273–285.
38. Silva, D. F.; Oliveira, A.; Pino, E. S.; Linardi, M.; Spinace, E. V. *J. Power Sources* **2007**, *170*, 303–307.
39. Sarma, L. S.; Lin, T. D.; Tsai, Y. W.; Chen, J. M.; Hwang, B. J. *J. Power Sources* **2005**, *139*, 44–54.
40. Li, L.; Xing, Y. C. *Energies* **2009**, *2*, 789–804.